

Cell-electronic sensing of particle-induced cellular responses†

Li Huang,^a Li Xie,^b Jessica M. Boyd^b and Xing-Fang Li^{*a,b}

Received 24th September 2007, Accepted 25th January 2008

First published as an Advance Article on the web 28th February 2008

DOI: 10.1039/b714384b

We report a new technique for the continuous and real-time measurement of microparticle-induced cellular responses using a real-time cell-electronic sensing (RT-CES) technology. The method involves the use of microelectrode-embedded microwells seeded with one of two lung cancer carcinoma cell lines (A549 and SK-MES-1), allowing for continuous measurements of impedance. The change in impedance that is automatically converted to the cell index is linearly correlated with the numbers of the seeding cells during the log phase, providing quantitative measurement of cytotoxicity. After 24 h of initial incubation in 96 microwells, the cultures are treated with microparticles, and changes in the cell index are monitored in real time. Multiple data, including dose response curves, IC_{50} (a concentration inhibiting 50% cell growth), and cell-specific and particulate-specific cell responses, are obtained from a single set of experiments. SK-MES-1 cells consistently showed more severe effects and lower IC_{50} values than A549 cells when they were treated with quartz particle suspensions. The different effects detected using the RT-CES technique were related to morphological change and apoptosis, supported by the scanning electronic microscopy and flow cytometry results. The method is further used to test the cytotoxicity of two PM_{10} standard reference materials of urban air dust and diesel particulates, demonstrating the potential application of this new technique for biomonitoring of air particulates.

Introduction

Cell-based sensing techniques and novel applications are actively developed by multidisciplinary researchers in bioanalytical chemistry, biochemistry, and biomedical engineering.¹ Unlike conventional biosensors that use attached affinity recognition molecules (e.g. antibodies), cell-based biosensors use living cells, which have a variety of native biomolecules on their surfaces. The use of the non-denatured molecules already naturally present in the cell membrane eliminates the tedious processes required for purification of affinity molecules while offering the potential for testing different types of substances and their *in vitro* toxicity. Cell-based sensors rely mainly on fluorescence and electronic detection for sensing various cellular events, while cell-electronic sensors are often based on impedance measurement.

Giaever and Keese first demonstrated electrical cell–substrate impedance sensing (ECIS) for real-time measurement of cellular events in 1984.² The ECIS technology has been used to monitor epithelial cell–matrix attachment,^{3,4} cell movement and

spreading,^{2,5} the endothelial response under fluid shear stress,⁶ the alteration of the barrier function of bronchial epithelial cells after antigen exposure,⁷ and the capacity of acetylcholinesterase (AChE) to increase the cell–substrate adhesion.⁸ The advances in the development and application of such cell impedance biosensors are summarized in a recent review.¹

Another technique called real-time cell-electronic sensing (RT-CES)^{9–11} uses similar principles as ECIS: the major difference between these two systems is the microelectrode design. The RT-CES system uses arrays of circle-on-line electrodes, whereas the ECIS consists of one large reference electrode and one or more small working electrodes that account for <0.1% of the surface area on the bottom of a well. Because the circle-on-line microelectrodes cover the entire bottom surface of a microwell in the RT-CES system, the majority of the cells are monitored and the signal reproducibility is improved. A number of applications of RT-CES, including measuring cell proliferation, cytotoxicity, and other cellular events, have been demonstrated.^{9–12} However, no study has demonstrated the application of the cell impedance sensing techniques for testing particulate matter. To this end, we will use the RT-CES system to develop a cell-microelectronic sensing method for the cytotoxicity testing of air particulates and to demonstrate the application of the cell-microelectronic sensing technique in biomonitoring of air quality.

Airborne particulate matter has been associated with a series of adverse health effects including cardiopulmonary disorders, and immunological and developmental toxicity.^{13–15} Assessment of air quality is often based on tedious and expensive analysis of chemical contaminants in air particulates. Little information is available on air quality monitoring based on the cytotoxicity of air particulates due to the lack of biomonitoring techniques.

^aEnvironmental Health Sciences, Department of Public Health Sciences, School of Public Health, University of Alberta, 10-102 Clinical Sciences Building, Edmonton, Alberta, Canada T6G 2G3.

E-mail: xingfang.li@ualberta.ca; Fax: 1-780-492-7800; Tel: 1-780-492-5094

^bDivision of Analytical and Environmental Toxicology, Department of Laboratory Medicine and Pathology, Faculty of Medicine and Dentistry, University of Alberta, 10-102 Clinical Sciences Building, Edmonton, Alberta, Canada T6G 2G3

† Electronic supplementary information (ESI) available: RT-CES sensing of methanol effects on A549 and SK-MES cell lines, and quartz particle interference in the RT-CES system and the acid phosphatase (AP) test. See DOI: 10.1039/b714384b

Reliable and rapid air quality screening methods are useful for human exposure and health risk assessment.

Conventional cytotoxicity assays are often based on colorimetric and fluorimetric measurements, such as the acid phosphatase (AP) test, neutral red intake assay, lactate dehydrogenase (LDH) assay, and 3-(4,5-dimethylthiazol-2-yl)-2,5-diphenyltetrazoliumbromide (MTT) assay.¹⁶ Cytotoxicity is measured based on the alteration of plasma membrane permeability, or the consequent release of cellular content into the cytoplasm or the inability of dead cells to metabolize various tetrazolium salts. Some of these methods involve multiple steps, which makes them time-consuming, and can provide data from only one time-point, which may result in missing information due to improper exposure time. To address these problems, we will explore an alternative label-free high-throughput method using the RT-CES technique. Two commonly used lung epithelial carcinoma cell lines (A549 and SK-MES-1) are chosen for sensing because of the association of air particulates with lung diseases. Because quartz-induced silicosis is well-documented,^{13–15} this method will be tested first with quartz particles of known physical and chemical properties, followed by more complex air particulate matter.

Experimental

Materials and reagents

Quartz particles (BCR[®] certified Reference Material) with two different average particle diameters, Q66 (0.35–3.50 μm) and Q70 (1.2–20.0 μm), were purchased from Sigma-Aldrich (Oakville, ON, Canada); the details on the characterization of these particles are available from the supplier. Urban dust (SRM 1649a) and diesel exhaust particle (SRM 2975) standard reference materials were purchased from the National Institute of Standards and Technology (Gaithersburg, MD, USA). The quartz particles were suspended in regular culture media before being added into the cultures. The urban dust and diesel exhaust particles were first dissolved in methanol to 200 and 50 mg mL^{-1} , respectively, followed by dilution to the desired concentration with regular culture media.

Cell culture conditions

Two human lung epithelial cells, A549 [CCL-185; American Type Culture Collection (ATCC), Manassas, VA, USA] and SK-MES-1 (HTB-58; ATCC) were cultured in standard 10 cm cell culture Petri dishes (Corning) at 37 °C with 5.5% CO₂ in RPMI 1640 medium (Sigma-Aldrich), supplemented with 10% fetal bovine serum (Sigma-Aldrich) and 1% penicillin/streptomycin (Invitrogen, Burlington, ON, Canada). When the cells reached 60% confluence, they were prepared for the subsequent RT-CES experiments as follows: the cells on the Petri dish were washed twice with 5 mL phosphate buffered saline (PBS) (pH 7.2), then 1 mL of 0.25% Trypsin/EDTA (Invitrogen) was added immediately followed by incubation for 3 min to detach the cells from the Petri dish. An aliquot of 5 mL RPMI 1640 medium was added and carefully mixed by gentle pipetting. The cells were collected by centrifugation for 3 min at 300 g. The cell pellets were prepared in fresh RPMI 1640 medium and then diluted to the desired population for the RT-CES experiments.

The numbers of cells were counted using a hemocytometer. A seeding population of 3000 cells well⁻¹ for A549 and 10 000 cells well⁻¹ for SK-MES-1 in a total volume of 150 μL well⁻¹ was used.

The RT-CES system

The real-time cell-electronic sensing (RT-CES) system (ACEA Biosciences, San Diego, CA, USA) has previously been described in detail.^{9–12} Briefly, this system is comprised of three components: an electronic sensor analyzer, a device station, and a 16-well E-plate. The circle-on-line electrode array is fabricated on glass slides (the bottom of the microwells), to which the cells are attached. These electrode sensor arrays detect changes in impedance in response to changes in cell attachment to the electrodes. The device station (analyzer) holds six E-plates in parallel, and it is placed inside a CO₂ (5.5%) incubator. Generally, A549 and SK-MES-1 cells in the microelectronic sensor wells grow readily under the common conditions described above. However, the content of CO₂ required for incubation is 5.5% rather than the 4% that is commonly used for mammalian cell culture. Changes in impedance corresponding to individual microwells are recorded in parallel, the signals are collected by the computer, and the impedance data are automatically converted to the cell index (CI) using a built-in calibration.

The cell index (CI) is a unitless value obtained from measuring the ratio of the electrical impedance in the presence of cells over that of the background. The equation of the CI is:

$$\text{CI} = \max_{i=1 \dots N} \left(\frac{R_{\text{cell}}(f_i)}{R_{\text{b}}(f_i)} - 1 \right)$$

where $R_{\text{cell}}(f)$ and $R_{\text{b}}(f)$ are the frequency-dependent electrode impedance with and without cells present, respectively.¹⁷ The parameter N represents the number of frequency points measured ($N = 3$ for 10 kHz, 25 kHz, and 50 kHz). Thus, CI is a quantitative measurement that reflects the numbers of cells attached to the microelectrode surface as well as the nature of the cells (*e.g.* cell morphology).

An initial population of 3000 A549 cells or 10 000 SK-MES-1 cells in a 150 μL volume was seeded separately into the individual microwells. CI values were automatically recorded once per hour. As the cells grew on top of the microelectrodes in the microwells, the CI increased. When the CI reached 1 (approximately 24 h of incubation), the culture medium was replaced with the particle suspension (200 μL) containing 0.03–0.8 mg mL^{-1} of the testing particles that were prepared in the culture medium. Control cells without treatment on the same E-plate were maintained in parallel. When the air particulates were tested, the controls treated with the same amounts of methanol were also included in addition to the cell controls without any treatment (Fig. S1, ESI†). The cultures were continuously monitored for 72–80 h. The CI data were used to calculate dose response curves using the Prism 4 software (Graphpad Software, San Diego, CA, USA).

Scanning electron microscope study

A549 cells and SK-MES-1 cells were treated with quartz particles (0.2 or 0.1 mg mL^{-1}) for 8 and 24 h, respectively. The

treated cells were pre-fixed in 2.5% glutaraldehyde in Millonig's buffer solution (pH 7.2) for 1.5 h at room temperature. The treated cells were then washed with the same buffer and were post-fixed with 1% of osmium tetroxide in the same buffer for 1.5 h. The samples were briefly washed with distilled water and dehydrated with a graded series of ethanol solutions (50, 70, and 90%, 10 min each grade) before the final two 10 min treatments with absolute ethanol. The fixed cells were then dried in a critical-point dryer (Seevac, Hialeah, FL, USA) at 31 °C for 5 min and mounted on stubs for sputter-coating (Edwards Vacuum, S150B, UK) with gold. The samples were examined with a Hitachi scanning electron microscope S-2500 (Tokyo, Japan).

Acid phosphatase (AP) test

The procedures of the AP test were similar to those described previously.¹⁶ A549 (5000 cells well⁻¹) and SK-MES-1 (10000 cells well⁻¹) cells were seeded on 96-well plates and treated with quartz particles for 24 h. After treatment, the medium was removed and the cells were washed with 200 μ L of PBS and 100 μ L of PBS containing 0.1 M sodium acetate (pH 5.5). Then 0.1% (v/v) Triton X-100 and *p*-nitrophenyl phosphate (Sigma-Aldrich) (10 mM) were added to the cells. After 1 h of incubation at 37 °C, NaOH (10 μ L of 1 M) was added to each well and the absorbance was measured at 405 nm using a microplate reader (Bio-Rad, Mississauga, ON, Canada).

Measurement of apoptotic cells using flow cytometry

Cell cycle analysis using flow cytometry was performed to determine the fraction of apoptotic cells.¹⁸ The cells were cultured in 5 cm Petri dishes. When the cells reached 60% confluence, the medium was replaced with 5 mL of the medium containing particle suspensions. After 24 h of treatment, the cells were

trypsinized, washed with PBS, and collected by centrifugation at 300 g for 3 min. The cell pellets were further washed with 5 mL ice-cold PBS and collected by centrifugation. The cells were then fixed in 70% ethanol overnight at 4 °C, followed by washing with 5 mL ice-cold PBS. The cells were collected and re-suspended in freshly prepared propidium iodide (PI) staining solution containing 0.1% Triton X-100 (VWR, Edmonton, AB, Canada), 100 μ g mL⁻¹ RNase A (Sigma-Aldrich), and 330 μ g mL⁻¹ PI (Sigma-Aldrich) in PBS. After incubation for 30 min at 37 °C in the dark, the stained cells were analyzed using a Becton and Dickinson FACScan™ (Mountain View, CA, USA). Data analysis was processed using the CellQuest™ software (Becton and Dickinson).

Results and discussion

We first established the optimum growth of A549 and SK-MES-1 cells on the microelectrodes in the microwells and evaluated the linear relationship between the cell index and cell numbers without particle treatment in order to develop a quantitative measurement of cell response to particles. A549 is a lung carcinoma cell line while SK-MES-1 is derived from a lung squamous cell carcinoma. There are no previous studies investigating particle toxicity in these cell lines; however, A549 cells have previously been shown to be more sensitive to benzo[a]pyrene.¹⁹ Fig. 1 shows the sensing curves of cell index *versus* incubation time, demonstrating typical cell growth curves of (A) A549 and (B) SK-MES-1 cells with initial seeding cell numbers ranging from 3000 to 20000 under optimized conditions for the RT-CES experiments. At time zero, no cells are attached to the microelectrodes so the cell index is zero. With increasing numbers of cells attaching to the microelectrodes over time, the cell index increases. During the log phase of the cell growth,

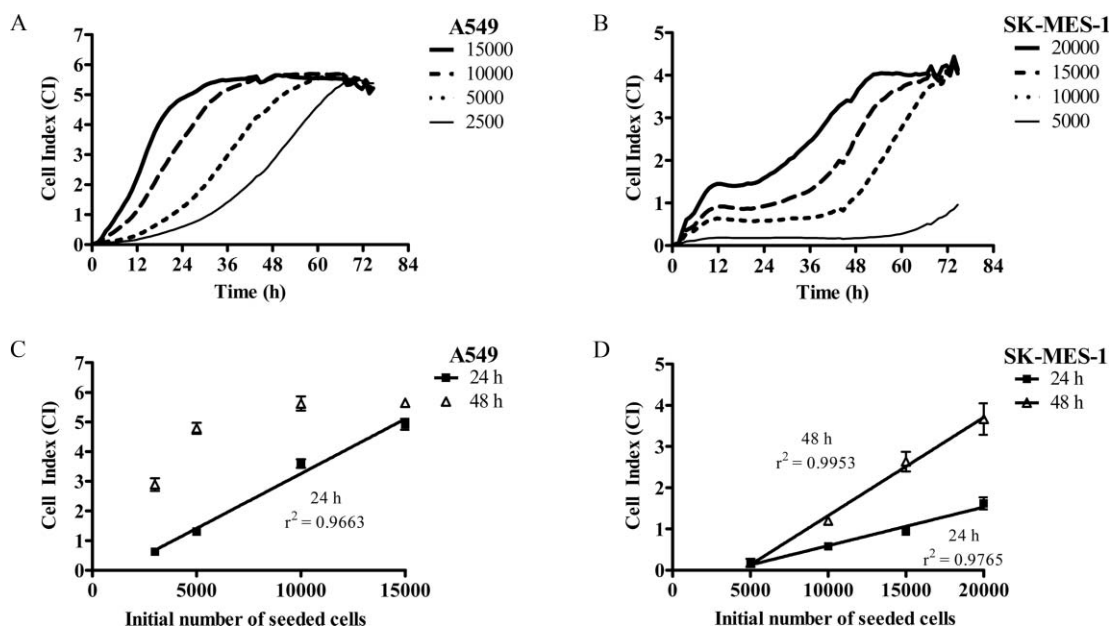


Fig. 1 Cell quantification on the RT-CES system. The top panels show the RT-CES growth curves of (A) A549 and (B) SK-MES-1 cells at different starting numbers ranging from 3000 to 20000. The slope of the growth curve indicates the different cell-specific growth rates. The lower panels show the relationship between the cell index (CI) and the numbers of initial seeding cells of (C) A549 and (D) SK-MES-1 at 24 or 48 h after plating.

the cell index increases in linear proportion to the number of cells with different seeding populations. In addition, a linear relationship between the cell index and the number of seeding cells is observed for both A549 at 24 h and SK-MES-1 cells during a period of 24–48 h, as shown in Fig. 1C and 1D. During the log phase, the linear relationship between the cell index and cell numbers is the basis for quantitative measurement of cell response to a substance. When the cells reach confluence, the microelectrodes in the wells are completely covered by the cells, and the cell index reaches a plateau. The time for the cell growth to reach a plateau is dependent on the number of initial seeding cells and the types of cells. A549 cells grow faster than SK-MES-1 cells; therefore, the A549 cells reach a plateau faster than SK-MES-1 cells with the same number of initial seeding cells.

Fig. 1 also demonstrates that it is important to use a proper number of initial seeding cells in order to establish a wider dynamic response range, as expected. When the number of seeding cells is too small, the cell index increases very slowly, resulting in low signal and low sensitivity. When the number of seeding cells is too large, the cells reach confluence rapidly, resulting in limited dynamic response range due to the saturation of the signal. This is probably the case for the results shown in Fig. 1C when A549 cells were incubated for 48 h. Different types of cells grow at different rates; therefore, the numbers of initial seeding cells required for various cell types are different. Based on the results in Fig. 1, the numbers of initial seeding cells for A549 and SK-MES-1 were chosen as 3000 and 10 000, respectively, for the following RT-CES studies.

Having established the RT-CES testing conditions, we investigated the capability of the RT-CES for testing particle-induced cytotoxicity. The pure quartz particles of known chemical and

physical properties that are associated with silicosis^{14,15} were tested on A549 and SK-MES-1 cells. Parallel experiments were performed on the six E-plates (16 microwells/plate). In order to control the cell population for testing different doses of particles, the seeding cells were allowed to grow until the cell index reached 1, which was approximately 24 h after seeding. The cells in individual microwells were then treated with an aliquot of 200 μL quartz particle (size range 0.35–3.5 μm) suspension at concentrations from 0.003 to 0.8 mg mL^{-1} and the cell index was continuously monitored for another 72 h for A549 cells and 80 h for SK-MES-1 cells. Fig. 2A and 2B show the growth curves of A549 and SK-MES-1, respectively, after the cells are treated with different concentrations of quartz particle suspensions. Fig. 2A and 2B demonstrate the concentration-dependent inhibitory effects of quartz particles on the growth of A549 and SK-MES-1 cells, respectively. These are the first set of experimental results showing that the cell-electronic sensing can measure dose-dependent cellular response to particles.

Dose response curves are generated based on viability, which is the relative cell index of the treated cells to that of the control cells at a given time. For example, Fig. 2C and 2D show the dose response curves after the cells were exposed to the particles for 12, 24, and 36 h. IC_{50} , a concentration causing 50% reduction in viability, is obtained from the dose response curves. After 12, 24, and 36 h of exposure, IC_{50} values for A549 cells are 1.97, 0.33, and 0.21 mg mL^{-1} , and IC_{50} for SK-MES-1 cells are 0.40, 0.06, and 0.04 mg mL^{-1} , respectively. The estimate of IC_{50} is accurate only during the log phase or within the linear range of the cell index *versus* cell numbers. Therefore, at 24 h after exposure to quartz particles, the IC_{50} values for A549 and SK-MES-1 cells that are 0.33 and 0.06 mg mL^{-1} , respectively,

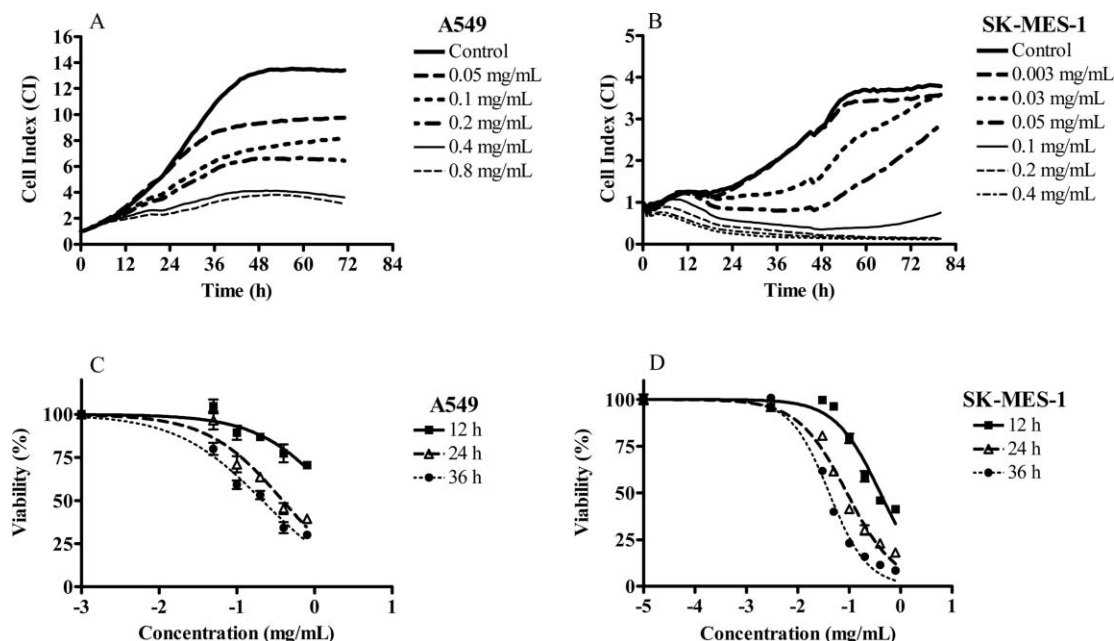


Fig. 2 Dynamic monitoring of cytotoxic response of A549 and SK-MES-1 cells to quartz particles (particle size 0.35–3.5 μm). The initial cells, 3000 for A549 cells and 10 000 for SK-MES-1 cells, were seeded into the 16 \times E-plates, and cell proliferation was monitored hourly. Once the cells reached the exponential growth phase, approximately 24 h later when the cell index increased to 1, they were treated with a quartz particle suspension at different concentrations as indicated. The control here indicates cells without quartz treatment. The cytotoxic response was then monitored dynamically. Figures A (A549) and B (SK-MES-1) show the RT-CES response curves; the time-point zero indicates the time when the quartz particle suspension was added into the E-plate. Figures C (A549) and D (SK-MES-1) show the dose response analysis of quartz-induced cytotoxicity.

are useful for comparison. These results show that SK-MES-1 cells are more sensitive than A549 cells to quartz particles. SK-MES-1 is a non-small lung cancer cell line while A549 is a lung carcinoma cell line. The difference of the two cell lines in response to particles or environmental contaminants has not been reported. Our results demonstrate that SK-MES-1 cells may serve as a more sensitive cell mode for screening the toxicity of particles.

To confirm the toxicity of quartz particles on the cells, we used scanning electron microscopy to examine the quartz particle-induced morphological changes in A549 and SK-MES-1 cells after treatment with 0.2 and 0.1 mg mL⁻¹ quartz particles, respectively. Fig. 3 shows the representative SEM results obtained at 8 and 24 h after treatment that show the distinct morphological changes on the A549 and SK-MES-1 cells. The SK-MES-1 cells started rounding up and shrinking in size at 8 h after quartz exposure and their size dwindled to 5 μm after 24 h compared to the size of the control cells, around 30 μm (Fig. 3A, 3B, 3C). The morphological change of the A549 cells was not as prominent as that of the SK-MES-1 cells (Fig. 3D, 3E, 3F). The A549 cells still retained their polyangular shape, and there was no obvious change in their size. However, cellular damage was observed, including the loss of normal microvilli on the surface and small lesions on the cells. Their well-maintained morphology allows the A549 cells to keep attaching to the electrodes and thus generate higher impedance. However, the degree of attachment of the SK-MES-1 cells decreased as they rounded up and shrank in size, and thus the cell index dropped more rapidly. The morphological changes at least partly explained the differences in the response curves measured by the RT-CES method.

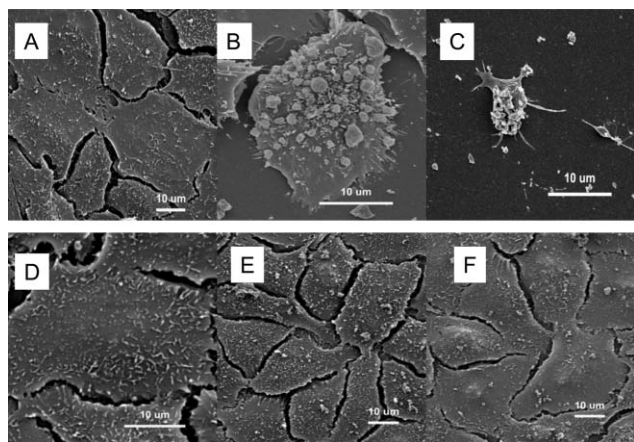


Fig. 3 Morphological changes observed by scanning electron microscopy. A549 and SK-MES-1 cells were treated with 0.2 and 0.1 mg mL⁻¹ quartz, respectively; the morphological changes were detected after 8 and 24 h of exposure. The top panels show the morphological changes of SK-MES-1 cells after quartz treatment: (A) control; (B) 8 h; (C) 24 h. The bottom panels demonstrate the changes of A549 cells: (D) control; (E) 8 h; (F) 24 h.

To confirm that the changes in the cell index detected by RT-CES (Fig. 2) are also associated with the changes in the number of live cells, we used flow cytometry to determine the percentage of apoptotic cells resulting from the quartz particle treatment. At 24 h after treatment with 0.2 and 0.4 mg mL⁻¹ of quartz

particles, the percentages of apoptotic cells in the treated SK-MES-1 cells increased to 35 and 89%, respectively, compared with 0.3% of apoptotic cells in the SK-MES-1 controls. Only 7 and 30% of treated A549 cells became apoptotic compared with 0.3% of A549 controls. The fact that quartz particles cause larger numbers of apoptotic SK-MES-1 cells than A549 cells is consistent with the RT-CES data that the cell index of SK-MES-1 cells reduced to near 0, whereas the cell index of the A549 cells reached a plateau after the same quartz treatment for up to 72 h after treatment. Cell index is an overall measure of cell attachment to the microelectrodes, which is dependent on the cell number and cell morphology. Both the flow cytometry (cell number) and SEM (morphology) data are consistent with the cell index results obtained from the RT-CES method, to monitor cell-specific toxicity resulting from particle treatment.

The results from the RT-CES, flow cytometry, and SEM demonstrate that SK-MES-1 cells are more sensitive to quartz particle treatment, and thus the following experiments were carried out with this cell line. SK-MES-1 cells were used to evaluate and compare the IC₅₀ obtained from the RT-CES method and the standard acid phosphatase (AP) assay. IC₅₀ values ($n = 3$) obtained by the RT-CES method (0.06 ± 0.01 mg mL⁻¹) were consistent with the values obtained by the AP assay (0.08 ± 0.03 mg mL⁻¹) using SK-MES-1 cells. The RT-CES method showed less variation compared to the AP tests, evident from the lower relative standard deviation of the RT-CES results (17%) compared to the AP assay results (37%). In addition, the interference of quartz particles on RT-CES measurements was also examined. As shown in Fig. S2 (ESI[†]), no interference was generated by quartz particles alone, without cells, when the RT-CES system was used, whereas AP tests show that the signal intensity of the particles is concentration-dependent with a correlation coefficient of 0.73 in the concentration range tested (0.05 – 0.6 mg mL⁻¹). At higher concentrations, the particles may interfere with the AP test.

The RT-CES technique was further used to test the cytotoxicity of particulate matter (PM): four types of particles, Q66, Q70, SRM 1649a, and SRM 2975, were tested on SK-MES-1 cells. Q66 and Q70 are quartz particles of different sizes. SRM 1649a is a standard reference material for urban dust mixture that contains at least 120 chemicals, including 44 or more polycyclic aromatic hydrocarbons (PAHs), 29 polychlorobiphenyl (PCB) congeners, chlorinated pesticides, and inorganic constituents.²⁰ SRM 2975 is a standard reference material for diesel exhaust particles (DEP). DEP are generated by the use of diesel engines in various industries, and form a major component of PM in many urban environment and occupational settings. DEP size is generally between fine and ultrafine PM upon emission into the atmosphere, *i.e.* <2.5 μm.²¹ These fine particles can remain in the air for a relatively long time and are associated with lung diseases and adverse health effects.²⁰ After 10 000 SK-MES-1 cells were seeded into individual microwells of the E-plates, the cell growth was continuously monitored. When the cell growth reached the cell index 1 (at 24 h after seeding), the cells were treated with different concentrations of the PM suspensions. The four types of particles inhibited the cell growth in a dose-dependent manner (data not shown), from which the IC₅₀ values were calculated. Fig. 4 shows the IC₅₀ values of the four types of PM to SK-MES-1 cells at 24, 36, and 48 h after exposure.

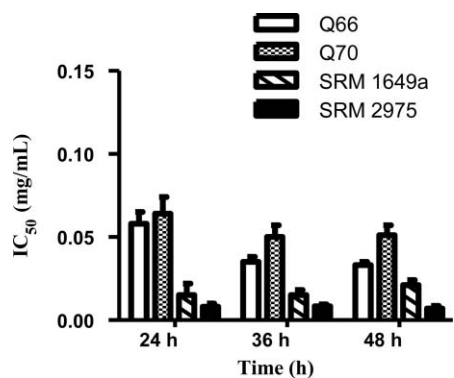


Fig. 4 IC₅₀ values of four types of particulate matter after exposure for 24, 36, and 48 h.

The IC₅₀ values show the relative toxicity in SK-MES-1 cells as SRM 2975 > SRM 1649a > Q66 > Q70. The IC₅₀ of diesel exhaust particle SRM 2975 is approximately eight times lower than that of quartz particles (Q70). Both SRM 1649a and SRM 2975 induce higher cytotoxicity than the simple quartz particles, suggesting that chemicals in the PM may be responsible. The successful detection of the cytotoxicity of SRMs demonstrates the potential application of this technique for the biomonitoring of air quality.

In summary, the RT-CES method based on electrical impedance measurement can provide real-time assessment of the cytotoxic activity induced by particulate matter without interference from the insoluble particles. The fully automated measurement without any labeling materials and reagents is potentially useful for large scale screening of particle-induced cytotoxicity. This provides a unique approach for biomonitoring of air quality as demonstrated by the SRM testing results.

Acknowledgements

This project was provided by grants from the Canadian Water Network, the Natural Sciences and Engineering Research Coun-

cil of Canada (NSERC), Alberta Health and Wellness, and an NSERC University Faculty Award (to X.-F. L.).

References

- 1 F. Asphahani and M. Zhang, *Analyst*, 2007, **132**, 835–841.
- 2 I. Giaever and C. R. Keese, *Proc. Natl. Acad. Sci. U. S. A.*, 1984, **81**, 3761–3764.
- 3 J. Gailit and R. A. Clark, *J. Invest. Dermatol.*, 1996, **106**, 102–108.
- 4 G. Ramirez-Icaza, K. A. Mohammed, N. Nasreen, R. D. Van Horn, J. A. Hardwick, K. L. Sanders, J. Tian, C. Ramirez-Icaza, M. T. Johnson and V. B. Antony, *J. Clin. Immunol.*, 2004, **24**, 426–434.
- 5 Z. Pei, C. R. Keese, I. Giaever, H. Kurzawa and D. E. Wilson, *Exp. Cell Res.*, 1994, **212**, 225–229.
- 6 N. DePaola, J. E. Phelps, L. Florez, C. R. Keese, F. L. Minnear, I. Giaever and P. Vincent, *Ann. Biomed. Eng.*, 2001, **29**, 648–656.
- 7 A. B. Antony, R. S. Tepper and K. A. Mohammed, *J. Allergy Clin. Immunol.*, 2002, **110**, 589–595.
- 8 K. V. Sharma, C. Koenigsberger, S. Brimijoin and J. W. Bigbee, *J. Neurosci. Res.*, 2001, **63**, 165–175.
- 9 K. Solly, X. Wang, X. Xu, B. Strulovici and W. Zheng, *Assay Drug Dev. Technol.*, 2004, **2**, 363–372.
- 10 N. DePaola, J. M. Atienza, N. Yu, S. L. Kirstein, B. Xi, X. Wang, X. Xu and Y. A. Abassi, *Assay Drug Dev. Technol.*, 2006, **4**, 597–607.
- 11 J. Z. Xing, L. Zhu, S. Gabos and L. Xie, *Toxicol. in Vitro*, 2006, **20**, 995–1004.
- 12 N. Yu, J. M. Atienza, J. Bernard, S. Blanc, J. Zhu, X. Wang, X. Xu and Y. A. Abassi, *Anal. Chem.*, 2006, **78**, 35–43.
- 13 S. V. Glinianaia, J. Rankin, R. Bell, T. Pless-Mullooli and D. Howel, *Epidemiology*, 2004, **15**, 36–45.
- 14 D. Buchanan, B. G. Miller and C. A. Soutar, *Occup. Environ. Med.*, 2003, **60**, 159–164.
- 15 World Health Organization Prevention and Control Exchange (PACE), *Hazard Prevention and Control in the Work Environment: Airborne Dust*, WHO Geneva 1999, WHO/SDE/OEH/99.14, Occupational and Environmental Health, WHO, Geneva, August 1999.
- 16 J. A. Cook and J. B. Mitchell, *Anal. Biochem.*, 1989, **179**, 1–7.
- 17 J. Z. Xing, L. Zhu, J. A. Jackson, S. Gabos, X. J. Sun, X. B. Wang and X. Xu, *Chem. Res. Toxicol.*, 2005, **18**, 154–161.
- 18 I. Nicoletti, G. Migliorati, M. C. Pagliacci, F. Grignani and C. Riccardi, *J. Immunol. Methods*, 1991, **139**, 271–279.
- 19 M. Ramet, K. Castren, K. Jarvinen, K. Pekkala, T. Turpeenniemi-Hujanen, Y. Soini, P. Paakko and K. Vahakangas, *Carcinogenesis*, 1995, **16**, 2117–2124.
- 20 T. Musafia-Jeknic, B. Mahadevan, C. Pereira and W. M. Baird, *Toxicol. Sci.*, 2005, **88**, 358–366.
- 21 C. P. Yu and G. B. Xu, *Res. Rep. Health Eff. Inst.*, 1987, **10**, 3–22.